Chapter 38
Application of MOBILE (*M*apping of *O*xygen *B*y *I*maging *L*ipids relaxation *E*nhancement) to Study Variations in Tumor Oxygenation

Bénédicte F. Jordan, Julie Magat, Florence Colliez, Elif Ozel, Anne-Catherine Fruytier, Valérie Marchand, Lionel Mignion, and Bernard Gallez

Abstract The aim of the study was to sensitively monitor changes in tumor oxygen using the MOBILE (mapping of oxygen by imaging lipids relaxation enhancement) technique. This method was applied in mammary tumor mouse models on an 11.7T Bruker MRI system. MOBILE was compared with functional imaging R_2*, R_1 of water and with pO_2 measurements (using EPR oximetry and O_2-dependent fluorescence quenching measurements). MOBILE was shown to be capable to monitor changes in oxygenation in tumor tissues.

38.1 Introduction

Tumor hypoxia is acknowledged as a major factor of resistance of solid tumors to treatment [1–3]. Quantitative follow-up of changes in tumor oxygenation can find relevant applications in radiation therapy planning [4, 5] as well as with regard to antiangiogenic and antivascular treatment optimization [6].

Direct quantitative methods, including Eppendorf microelectrodes [7], electron paramagnetic resonance (EPR) oximetry [8], ^{19}F relaxometry [9], or Overhauser-enhanced magnetic resonance imaging (MRI) [10], either are invasive or require the injection of a reporter probe and are currently not clinically applicable. Nowadays, the clinically available armamentarium for this purpose only includes radiolabeled nitroimidazoles detected by positron emission tomography (PET) which prominently accumulate in hypoxic areas, thereby acting as potential markers for tissue hypoxia [11]. Endogenous sources of contrast in MRI include variations of T_1

B.F. Jordan • J. Magat • F. Colliez • E. Ozel • A.-C. Fruytier • V. Marchand
L. Mignion • B. Gallez, Ph.D. (✉)
Biomedical Magnetic Resonance Research Group, Louvain Drug Research Institute,
Université Catholique de Louvain, Av.Mounier 73.40, Brussels 1200, Belgium
e-mail: Bernard.gallez@uclouvain.be

S. Van Huffel et al. (eds.), *Oxygen Transport to Tissue XXXV*, Advances in Experimental Medicine and Biology 789, DOI 10.1007/978-1-4614-7411-1_38,

(longitudinal relaxation rate) and T_2* (effective transversal relaxation rate) values in tissue [12]. T_1 discloses sensitivity to dissolved oxygen, which acts as a T_1-shortening paramagnetic contrast agent [13]; T_2* is sensitive to the relative deoxyhemoglobin/oxyhemoglobin (Hb/HbO_2) ratio in vessels [14]. T_2* mapping, also referred to as functional MR imaging or "BOLD" (blood oxygen level dependent) imaging, is sensitive to variations in oxygenation in the vascular compartment and has been successfully applied to monitor changes in tissue oxygenation [15, 16]. However, BOLD-MRI has also demonstrated significant limitations in terms of quantitative relationships between response signal intensity and true changes in tissue pO_2 and is sensitive to changes in total hemoglobin content [17–19]. Recently, changes in tissue oxygen concentrations have been shown to produce changes in relaxation rate R_1 (=1/T_1) of water [20–22]. Unfortunately, the technique still suffers from insufficient sensitivity.

In our lab, we have developed an MR method for mapping variations in oxygenation based on changes in relaxation properties of the tissue lipids, which we called "MOBILE," for mapping of oxygen by imaging lipids relaxation enhancement [23]. In vitro, a gain in sensitivity (compared with water) was demonstrated and evaluated to a factor of 7.5 in pure oil and 2.1 and 11.4 in tissue homogenates corresponding to two distinct common lipid peaks with a chemical shift of ~1.3 (fatty acid chains) and ~4.0 ppm (glycerol backbone of triglycerides), respectively [23]. In vivo we also demonstrated the feasibility in several tissues on preclinical and clinical studies. In the present study, our goal was to apply the MOBILE technique to monitor tumor oxygenation during carbogen challenge and to compare this technique with two quantitative measurements of tumor pO_2 (invasive MR compatible fiber-optic fluorescence quenching probes, OxyLite™, and EPR oximetry). We also compared MOBILE to two currently used MR parameters, namely, R_2* and R_1 of water.

38.2 Methods

Syngeneic NT2 and MDA human mammary tumor cells were injected subcutaneously (implanted orthotopically) into the right upper mammary fat pad of 6-week-old FVB/N or nude NMRI female mice (Janvier), respectively (n=5/model). Tumors were analyzed when reaching 6 mm in diameter. Animals were anesthetized by inhalation of isoflurane (Forene; Abbot, England; mixed with 21 % oxygen, 1.5 l/h). Respiration rate and body temperature (37.0 °C +/−1.0 °C) were monitored. Studies were undertaken in accordance with the national and local regulations of the ethical committee (agreement number LA 1230467).

Experiments were performed with an 11.7T MRI system (Bruker, BioSpec; Ettlingen, Germany) and with a quadrature volume coil (inner diameter of 40 mm). Three MR measurements of each type (R_1 H_2O, R_1 lipids, R_2*) were acquired sequentially and repeated three times during air breathing. Then, breathing gas was switched to carbogen. Respiratory triggering was employed to avoid motion artifacts. We used the OxyLite™ fiber-optic microprobes for continuously monitoring tumor oxygenation simultaneously with MRI [24]. Independent experiments

were also performed to compare MOBILE with EPR oximetry using a similar breathing challenge.

A segmented IR FISP [25] (inversion-recovery fast imaging with steady-state precession) sequence (SSFP FID mode) was used to acquire parametric images of T_1 relaxation time. The acquisition parameters were TR/TE/FA/BW/matrix = 4 ms/1.2 ms/5°/100 kHz/64 × 64, four segments, and a total acquisition time of 1 min 20 s. For the total proton experiment, a series of 100 images were acquired (spaced by a scan repetition time TR = 120 ms) with a slice thickness of 1 mm. For the lipid experiments, we first evaluated the frequency difference in hertz between water and lipid peaks in the ^{1}H spectrum with a single pulse sequence. These offsets were then used as an imaging frequency offset in the same IR FISP protocol. Typically, the lipid peak of interest was approximately 4.0 ppm for tumor as identified experimentally [26]. We added a π/2 hermite saturation pulse to cancel the water signal. A series of 40 images (spaced by scan repetition time TR = 100 ms) with a slice thickness of 3 mm were acquired. Then, images were fitted using a homemade program in Matlab (the MathWorks, Inc., Natick, MA, USA) to determine the T_1 relaxation in regions of interest (ROIs). Raw data were filtered so as to disregard nonrelevant fits with a T_1 error/T_1 > 30 %. T_1 values were then calculated from the effective T_1* values measured experimentally [27]. Finally, R_1 ($1/T_1$) data were filtered according to the calibration curves obtained in vitro from tissue extracts (R_1 0 % O_2 < measured R_1 < R_1 100 % O_2).

For T_2* measurements, a multi-gradient echo (MGE) sequence was performed with eight echoes (between 3.5 and 31.5 ms) with a total acquisition time of 4 min 48 s. A 256 × 256 matrix was used with TR/flip angle/slice thickness = 1,500 ms/30°/1 mm.

In vivo tumor pO_2 was monitored using electron paramagnetic resonance (EPR) oximetry using charcoal as the oxygen-sensitive probe [8]. EPR spectra were recorded using a 1.1 GHz EPR spectrometer (Magnettech, Berlin, Germany). Calibration curves were made by measuring the EPR line width as a function of the pO_2. Mice were injected in the center of the tumor using the suspension of charcoal (100 mg/ml, 60 µl injected). The tumor under study was placed in the center of the extended loop resonator whose sensitive volume extends 1 cm into the tumor mass. The pO_2 measurements correspond to an average of pO_2 values in this volume of the NT2 tumor models. Charcoal was injected 24 h before experiments. MOBILE and EPR measures were performed the same day, and it was verified that charcoal did not perturb MOBILE or T_1 MRI measurements.

Paired *t*-tests (carbogen versus air breathing), linear fits, and Pearson correlations ($p < 0.05$ (*), $p < 0.01$ (**), or $p < 0.001$ (***) were considered significant) were performed using the GraphPad software.

38.3 Results and Discussion

The basal pO_2 measured with OxyLite in MDA tumors ranged from 2 to 25 mmHg (mean of $pO_2 = 14.15 \pm 5.46$ mmHg), whereas basal pO_2 in NT2 tumors was between 35.5 and 46.7 mmHg (mean of $pO_2 = 37 \pm 0.8$ mmHg). Tumor oxygenation was

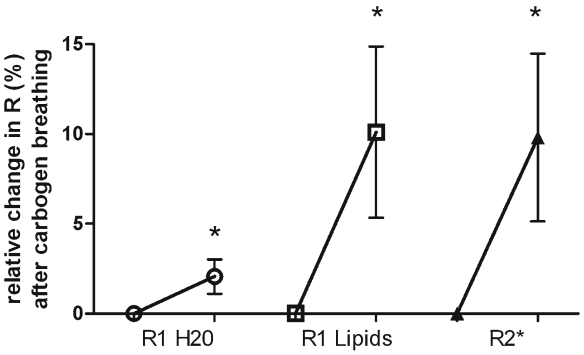

Fig. 38.1 Pooled results of MDA and NT2 tumors ($n=12$). Relative changes over the whole tumors in relaxation times under air and carbogen breathing conditions for global R1 (water), R1 of lipids, and R2* [R = 1/T]. Note the higher change in R1 of lipids versus global R1 in response to carbogen breathing

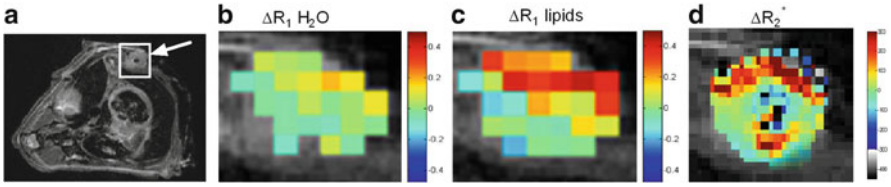

Fig. 38.2 Anatomical transversal MR image of a mouse with an MDA tumor (shown by the *arrow*) with the OxyLite tip (*black spot*) at the center of the tumor (**a**). Typical maps of changes in relaxation times in response to carbogen breathing (**b**, **c**, **d**) (Δ = R carbogen − R air). Color scales highlight the higher sensitivity of the MOBILE technique with a higher proportion of "hot" colors (**c**)

increased in the majority of the tumors (7/8) under carbogen breathing conditions. After carbogen breathing, MDA and NT2 tumors reached a pO_2 around 41.2 ± 2.3 mmHg and 87.7 ± 14.1 mmHg, respectively. Mean relative changes in relaxation rates with respect to the hyperoxic challenge were compared (pooled results for both tumor models) between R_1 H_2O, R_1 lipids and R_2*, with relative changes of 2.1 ± 1.0 % ($p<0.05$; ΔR_1 H_2O), 10.1 ± 4.8 % ($p<0.05$; ΔR_1 lipids), and 9.8 ± 4.6 % ($p<0.05$; ΔR_2*) (Fig. 38.1). Although values are rather dispersed, an increase by a factor of 4.8 was achieved for R_1 lipids compared to R_1 H_2O. The larger dispersion of the data obtained using R_1 lipids compared to R_1 H_2O is explained by the fact that MOBILE is more sensitive to changes in oxygenation than R_1 H_2O and that the tumor is highly heterogeneous (Fig. 38.2): areas with a large change in pO_2 will present a larger change in R_1 lipids compared to R_1 H_2O, while areas with no change in pO_2 will have no change in R_1 (lipids or water). As tumors are heterogeneous (mixture of areas with response and areas without response to hyperoxic challenge), the effect of change in oxygenation leads to a larger distribution in the recorded values when using a method that is highly sensitive. The tip of the OxyLite™ probe could be localized on the MR images (Fig. 38.2a). Typical maps of

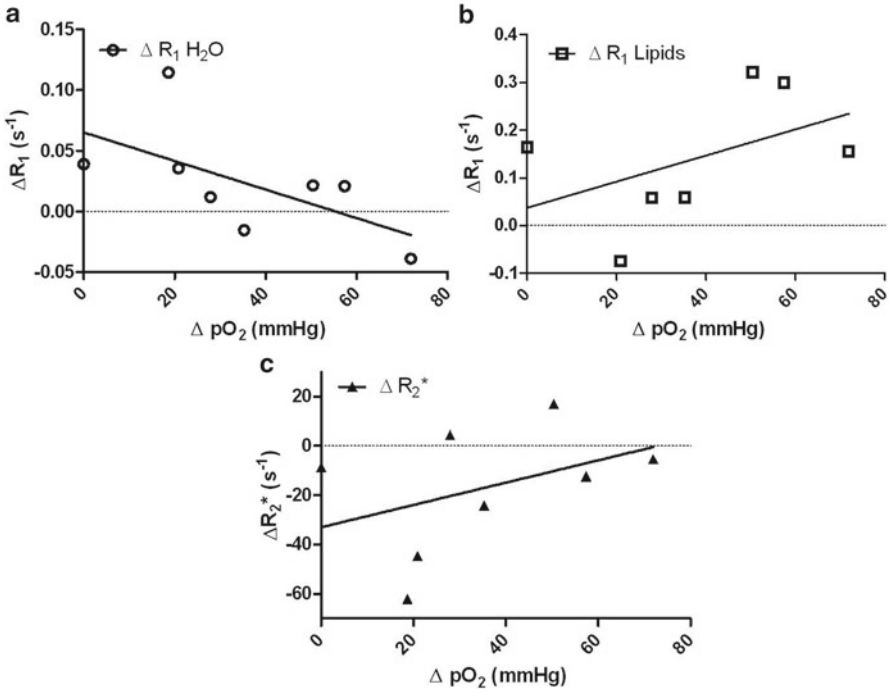

Fig. 38.3 Relation between the quantitative change in tumor pO_2 (assessed by OxyLite probes) and the corresponding changes in relaxation times: global R1 (**a**), R1 of lipids (**b**), and R2* (**c**). Note the positive trend for R1 of lipids

the relative difference in relaxation rates before and during the carbogen challenge were generated in order to compare the sensitivity of the R_1 of lipids (MOBILE), R_1 H_2O, and R_2* methods (Fig. 38.2b–d), indicating that ΔR_1 lipids are more sensitive (more red pixels) than ΔR_1 H_2O on the same tumor. It is possible to compare the quantitative values obtained by fluorescence quenching and the MR relaxation values obtained in the sensitive region of the probe (3*3 pixels with the exclusion of the central pixel, Fig. 38.3a–c), similarly to previously published comparisons between R_2* and pO_2 changes [17]. Some trends were found between ΔR_1 lipids and ΔpO_2, presenting a positive linear fit with a slope of 0.0027 ± 0.0023 ($r^2 = 0.22$, $p = 0.11$). In contrast, ΔR_1 H_2O presented a negative slope versus ΔpO_2 (-0.0012 ± 0.0006; $r^2 = 0.37$, $p = 0.28$), and ΔR_2* presented a positive slope (0.4527 ± 0.4120; $r^2 = 0.17$, $p = 0.31$), while this was expected to be negative (i.e., pO_2 is reported to be linked to $T_2^* = 1/R_2^*$). In a parallel study, we compared EPR oximetry and R_1 lipids and R_1 H_2O in the NT2 tumor model. The basal pO_2 was 8.4 ± 1.1 mmHg and reached 26.1 ± 6.1 mmHg after carbogen breathing. The correlation between R_1 H_2O and pO_2 was not significant ($p = 0.8611$, positive linear fit 0.000409 ± 0.002241; $r^2 = 0.005529$) (Fig. 38.4), while a positive linear significant correlation was found between R_1 lipids and pO_2 (0.01744 ± 0.00656; $r^2 = 0.5407$, $p = 0.0376$) (Fig. 38.4).

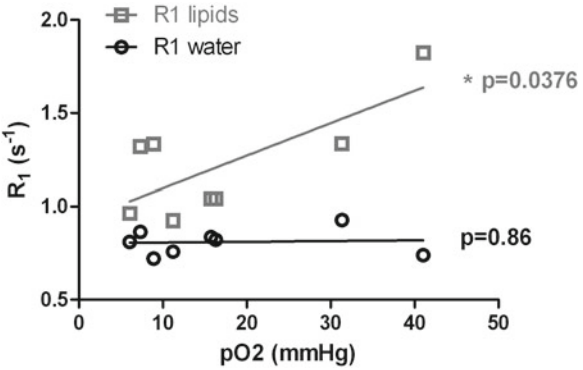

Fig. 38.4 Correlation between global pO_2 measures with global R1 values and lipids R1 values

Overall, these data show that MOBILE is sensitive to changes in tumor oxygenation. Correlations between data sets from MOBILE and direct O_2 measurements suggested that R_1 lipids were significantly correlated with pO_2 measured by EPR. Using OxyLite, we found a positive (but nonsignificant) fit between ΔR_1 lipids and ΔpO_2. Differences observed between EPR and OxyLite measurements can be explained by the difference in the volume sampled, as OxyLite interrogates a very small volume while EPR provides pO_2 measurements over the whole tumor.

Also, ΔR_2*, which was expected to be negatively correlated to pO_2, showed an apparently paradoxical positive fit versus ΔpO_2, thereby emphasizing the multiplicity and complexity of the response of R_2* to changes in oxygenation and perfusion that can be highly dependent on micro/macrovasculature functional parameters [28]. Therefore, information provided by the two relaxation parameters should be complementary. Also, oxygen-enriched gases inhalation was used as a technique to modulate tumor oxygenation. However, actual effects of such gases might vary from one tissue to the other, e.g., according to the presence or absence of CO_2 (i.e., for carbogen). This may explain the dispersion of the results, where tissue tumor heterogeneity is high. MOBILE presents the advantage of allowing longitudinal studies. Interestingly, the short acquisition time (1 min 20 s) of the MOBILE sequence should allow the follow-up of acute hypoxia in tumors in a quantitative and dynamic way, similarly to previous work using ^{19}F-relaxometry or EPR oximetry [29, 30].

38.4 Conclusion

In conclusion, these initial studies suggest that MOBILE has the potential to provide a noninvasive method for obtaining measurements of the variations in tumor oxygenation. Further studies on other tumor models are needed to evaluate if changes in R_1 lipids are quantitatively reflecting changes in pO_2.

Acknowledgments This study was supported by grants from the Belgian National Fund for Scientific Research (FNRS), the Joseph Maisin Foundation, the Saint-Luc Foundation, the "Actions de Recherches Concertées-Communauté Française de Belgique, grant no. ARC 09/14-020," and the "Pôle d'Attraction Interuniversitaire, PAI VI (P6/38)", and the 2011 ISMRM Seed Grant. B.F.J. and P.D.C. are Research Associates of the FNRS and O.F. is a Senior Research Associate of the FNRS.

References

1. Tatum JL, Kelloff GJ, Gillies RJ et al (2006) Hypoxia: importance in tumor biology, noninvasive measurement by imaging, and value of its measurement in the management of cancer therapy. Int J Radiat Biol 82(10):699–757
2. Wilson WR, Hay MP (2011) Targeting hypoxia in cancer therapy. Nat Rev Cancer 11(6): 393–410
3. Begg AC, Stewart FA, Vens C (2011) Strategies to improve radiotherapy with targeted drugs. Nat Rev Cancer 11(4):239–253
4. Rodrigues LM, Howe FA, Griffiths JR, Robinson SP (2004) Tumor R2* is a prognostic indicator of acute radiotherapeutic response in rodent tumors. J Magn Reson Imaging 19(4):482–488
5. Elas M, Bell R, Hleihel D et al (2008) Electron paramagnetic resonance oxygen image hypoxic fraction plus radiation dose strongly correlates with tumor cure in FSa fibrosarcomas. Int J Radiat Oncol Biol Phys 71(2):542–549
6. Robinson SP, Kalber TL, Howe FA et al (2005) Acute tumor response to ZD6126 assessed by intrinsic susceptibility magnetic resonance imaging. Neoplasia 7(5):466–474
7. Milosevic M, Fyles A, Hedley D, Hill R (2004) The human tumor microenvironment: invasive (needle) measurement of oxygen and interstitial fluid pressure. Semin Radiat Oncol 14(3): 249–258
8. Gallez B, Baudelet C, Jordan BF (2004) Assessment of tumor oxygenation by electron paramagnetic resonance: principles and applications. NMR Biomed 17(5):240–262
9. Yu JX, Cui W, Zhao D, Mason RP (2008) Non-invasive physiology and pharmacology using 19F magnetic resonance. In: Tressaud A, Haufe G (eds) Fluorine and health. Elsevier, Amsterdam, pp 197–276
10. Matsumoto S, Yasui H, Batra S et al (2009) Simultaneous imaging of tumor oxygenation and microvascular permeability using Overhauser enhanced MRI. Proc Natl Acad Sci USA 106(42):17898–17903
11. Sharma R (2011) Nitroimidazole radiopharmaceuticals in bioimaging: part I: synthesis and imaging applications. Curr Radiopharm 4(4):361–378
12. Pacheco-Torres J, López-Larrubia P, Ballesteros P, Cerdán S (2011) Imaging tumor hypoxia by magnetic resonance methods. NMR Biomed 24(1):1–16
13. Matsumoto K, Bernardo M, Subramanian S et al (2006) MR assessment of changes of tumor in response to hyperbaric oxygen treatment. Magn Reson Med 56(2):240–246
14. Ogawa S, Lee TM, Kay AR, Tank DW (1990) Brain magnetic resonance imaging with contrast dependent on blood oxygenation. Proc Natl Acad Sci USA 87(24):9868–9872
15. Robinson SP, Howe FA, Griffiths JR (1995) Noninvasive monitoring of carbogen-induced changes in tumor blood flow and oxygenation by functional magnetic resonance imaging. Int J Radiat Oncol Biol Phys 33(4):855–859
16. Baudelet C, Ansiaux R, Jordan BF, Havaux X, Macq B, Gallez B (2004) Physiological noise in murine solid tumours using T2*-weighted gradient-echo imaging: a marker of tumour acute hypoxia? Phys Med Biol 49(15):3389–3411
17. Baudelet C, Gallez B (2002) How does blood oxygen level-dependent (BOLD) contrast correlate with oxygen partial pressure (pO_2) inside tumors? Magn Reson Med 48(6):980–986

18. McPhail LD, Robinson SP (2010) Intrinsic susceptibility MR imaging of chemically induced rat mammary tumors: relationship to histologic assessment of hypoxia and fibrosis. Radiology 254(1):110–118
19. Howe FA, Robinson SP, McIntyre DJ, Stubbs M, Griffiths JR (2001) Issues in flow and oxygenation dependent contrast (FLOOD) imaging of tumours. NMR Biomed 14(7–8):497–506
20. O'Connor JP, Jackson A, Buonaccorsi GA et al (2007) Organ-specific effects of oxygen and carbogen gas inhalation on tissue longitudinal relaxation times. Magn Reson Med 58(3): 490–496
21. O'Connor JP, Naish JH, Parker GJ et al (2009) Preliminary study of oxygen-enhanced longitudinal relaxation in MRI: a potential novel biomarker of oxygenation changes in solid tumors. Int J Radiat Oncol Biol Phys 75(4):1209–1215
22. Winter JD, Estrada M, Cheng HL (2011) Normal tissue quantitative T1 and T2* MRI relaxation time responses to hypercapnic and hyperoxic gases. Acad Radiol 18(9):1159–1167
23. Jordan BF, Magat J, Colliez F et al (2012) Mapping of oxygen by imaging lipids relaxation enhancement: a potential sensitive endogenous MRI contrast to map variations in tissue oxygenation. Magn Reson Med. doi:10.1002/mrm.24511 (in press)
24. Jordan BF, Cron GO, Gallez B (2009) Rapid monitoring of oxygenation by 19F magnetic resonance imaging: simultaneous comparison with fluorescence quenching. Magn Reson Med 61(3):634–638
25. Scheffler K, Henning J (2001) T1 quantification with inversion recovery TrueFISP. Magn Reson Med 45(4):720–723
26. Delikatny EJ, Chawla S, Leung DJ, Poptani H (2011) MR-visible lipids and the tumor microenvironment. NMR Biomed 24(6):592–611
27. McGrath DM, Naish JH, O'Connor JP et al (2008) Oxygen-induced changes in longitudinal relaxation times in skeletal muscle. Magn Reson Imaging 26(2):221–227
28. Kim KA, Park MS, Kim IS et al (2012) Quantitative evaluation of liver cirrhosis using T1 relaxation time with 3 tesla MRI before and after oxygen inhalation. J Magn Reson Imaging 36(2):405–410
29. Magat J, Jordan BF, Cron G, Gallez B (2010) Noninvasive mapping of spontaneous fluctuations in tumor oxygenation using 19F MRI. Med Phys 37(10):5434–5441
30. Matsumoto S, Yasui H, Mitchell JB, Krishna MC (2010) Imaging cycling tumor hypoxia. Cancer Res 70(24):10019–10023